

## ELECTROMAGNETIC PROCESSES IN RELATIVISTIC HEAVY ION COLLISIONS

C.A. BERTULANI<sup>1</sup> AND G. BAUR

*Institut für Kernphysik, Kernforschungsanlage Jülich, D-5170 Jülich, West Germany*

Received 24 February 1986

(Revised 21 April 1986)

**Abstract:** Electromagnetic effects in relativistic heavy ion collisions with impact parameter larger than the sum of the nuclear radii are studied using the virtual photon method. With increasing value of the relativistic parameter  $\gamma$  the hardness of the virtual photon spectrum increases. This leads to interesting new effects which will also have to be considered in the design of future relativistic heavy ion machines and experiments. The excitation of high-lying giant E1 and E2 multipole resonances is calculated as well as electromagnetic pion production. Coulomb bremsstrahlung is calculated and compared to the bremsstrahlung emitted in the more violent central nuclear collisions. K-shell ionization and electron-positron pair production is studied. The latter process has a very large cross section for heavy ions and contributes significantly to the stopping power of relativistic heavy ions in a dense medium.

### 1. Introduction

Due to the Lorentz contraction, the electromagnetic field of a relativistic charged projectile as seen from a target (or vice-versa) increases with the relativistic parameter  $\gamma = (1 - v^2/c^2)^{-1/2}$ . Also, the time duration of their electromagnetic interaction decreases with  $1/\gamma$  [see e.g. ref. <sup>1</sup>]. This situation corresponds to the presence of virtual photons with high energies, the intensities of the virtual photon spectrum being proportional to  $Z^2$ . This means that particularly strong sources of virtual photons are provided by heavy ions. Since the short range nuclear effects are restricted geometrically to an area of  $\pi(R_1 + R_2)^2$  in a collision, the importance of electromagnetic effects, due to their long range and to the Lorentz contraction, will increase with  $\gamma$  and large impact parameters will contribute to the cross sections.

It is the aim of this paper to explore, by means of the virtual photon theory [see refs. <sup>1-7</sup>], the electromagnetic effects in relativistic heavy ion collisions. The virtual photon theory is outlined in sect. 2. It forms a reliable basis for the effects to be studied further. Since relativistic heavy ion accelerators are in operation and are being built with increasing energy, we feel that it is important to study such effects which can be predicted quite directly due to our good understanding of the electromagnetic interaction. These processes may be a source of background for the

<sup>1</sup> On leave of absence from Federal University of Rio de Janeiro, Brazil.

nuclear interactions one is mainly interested in (like the formation and the possible signatures for a quark-gluon plasma) [see e.g. ref. <sup>8</sup>]. But they are also interesting to study by themselves.

In low-energy nuclear physics Coulomb excitation plays a key role in the study of collective low-lying states and multiple excitation has become a powerful tool to extract information about these states. In relativistic Coulomb collisions it is possible to excite high-lying states, like the giant E1 and E2 resonances, due to the short duration of the electromagnetic interaction. However, we expect multiple excitation effects to be generally of less importance. This will be discussed in sect. 3. At even higher values of the relativistic parameter  $\gamma$ , it will be possible to produce pions through the excitation of  $\Delta$ -resonances in the nuclei.

In sect. 4 the emission of bremsstrahlung will be discussed. The effect of the virtual photons on the electron cloud will also be an interesting subject in relativistic ion studies. We calculate the ionization of electrons, K-shell ionization being most important. This is done in sect. 5. A very important process will also be the creation of electron-positron pairs: with its large cross section it will be a major cause of the stopping power of relativistic heavy ions, as is shown in sect. 6. Our conclusion and an outlook are given in sect. 7. Part of this work was reported earlier <sup>9</sup>) in a preliminary form.

## 2. Virtual photon theory

A standard way of studying the electromagnetic effects in relativistic heavy ion collisions (RHIC) is the use of the Weizsäcker-Williams approximation <sup>1-4</sup>) which properly accounts for the electric dipole excitation. But the inclusion of other multipolarities of excitation is also very important and recently an extension of the Weizsäcker-Williams method to include all other multipolarities was accomplished <sup>5,6</sup>). In this theory the excitation cross section of one nucleus by an energy amount  $\hbar\omega$  due to the electromagnetic interaction with the other nucleus is given by

$$\sigma_C = \sum_{\pi l} \int n_{\pi l}(\omega) \sigma_{\gamma}^{\pi l}(\omega) \frac{d\omega}{\omega}, \quad (2.1)$$

where  $n_{\pi l}(\omega)$  is the equivalent number of photons with the frequency  $\omega$  (also called by virtual photon numbers) of the electric ( $\pi = E$ ) or magnetic ( $\pi = M$ ) radiation and multipolarity  $l$ . They are given in an analytical form in ref. <sup>6</sup>). The functions  $\sigma_{\gamma}^{\pi l}(\omega)$  are the photonuclear absorption cross sections for the excitation energy  $\hbar\omega$ .

We shall study here only the effects of the most important multipolarities, namely the electric dipole E1, the magnetic dipole M1 and the electric quadrupole E2 interactions. We quote from ref. <sup>6</sup>)

$$n_{E1}(\omega) = Z^2 \alpha \frac{2}{\pi} \left( \frac{c}{v} \right)^2 \left[ \xi K_0 K_1 - \frac{v^2 \xi^2}{2c^2} (K_1^2 - K_0^2) \right], \quad (2.2a)$$

$$n_{E2}(\omega) = Z^2 \alpha \frac{2}{\pi} \left(\frac{c}{v}\right)^4 \left[ 2 \left(1 - \frac{v^2}{c^2}\right) K_1^2 + \xi \left(2 - \frac{v^2}{c^2}\right)^2 K_0 K_1 + \frac{\xi^2}{2} \left(\frac{v}{c}\right)^4 (K_0^2 - K_1^2) \right], \quad (2.2b)$$

$$n_{M1}(\omega) = Z^2 \alpha \frac{2}{\pi} \left[ \xi K_0 K_1 - \frac{\xi^2}{2} (K_1^2 - K_0^2) \right], \quad (2.2c)$$

where  $Z$  is the projectile charge (for target excitations) or the target charge (for projectile excitations),  $\alpha$  is the fine-structure constant,  $v$  is the relative velocity of the ions,  $c$  is the velocity of light, and  $K_n$  are the modified Bessel functions of  $n$ th order as functions of the adiabaticity parameter

$$\xi = \frac{\omega R}{\gamma v}. \quad (2.3)$$

In the above formula  $\gamma$  is the relativistic Lorentz factor

$$\gamma = \left(1 - \frac{v^2}{c^2}\right)^{-1/2} \quad (2.4)$$

and  $R$  is the sum of the two nuclear radii.

In ref. <sup>5</sup>) it is suggested to improve upon expression (2.3) by using  $\xi = (\omega/\gamma v) \times (R + \frac{1}{2} \pi Z_1 Z_2 e^2 / m_0 v^2 \gamma)$  where  $m_0$  is the reduced mass of the two nuclei, in order to take into account nuclear recoil effects in an approximate way. This modification, which becomes important for lower values of  $\gamma$ , will be of minor importance for the purpose of this paper. Therefore we prefer to drop this recoil correction at present. Another problem is related to the choice of the minimum impact parameter, which is not too well defined due to the diffuseness of the nuclear surface, which will give rise to Coulomb-nuclear interference effects which are not considered here. Perhaps, it will become possible in future relativistic heavy ion experiments to determine the impact parameter in a Coulomb collision by a measurement of the scattering angle or the recoil energy of one of the two nuclei. This can lead to more exact studies of relativistic electromagnetic collisions.

For  $1 \leq \gamma \leq 2$ , corresponding to the intermediate energy regime of some hundreds of MeV/nucleon, then  $n_{E2} \gg n_{E1} \gg n_{M1}$ . But for  $\gamma \gg 1$ , corresponding to the ultrarelativistic regime, then all virtual photon numbers are equal to (except for the excitation of extremely low-lying states, satisfying the relationship  $\omega R/c \ll 1$ )

$$n_{\pi l} = Z^2 \alpha \frac{1}{\pi} \ln \left[ \left(\frac{\delta}{\xi}\right)^2 + 1 \right] \quad (2.5)$$

with  $\delta = 0.681085 \dots$ . The physical reason for these two different behaviours of the virtual photon numbers is the following. The electric field of a charged particle moving at low energies is approximately radial and the lines of forces of the field are isotropically distributed, with their relative spacing increasing with the radial distance. When interacting with a target of finite dimension the non-uniformity of

the field inside the target is responsible for the large electric quadrupole interaction between them. The same lines of force of an ultrarelativistic ( $\gamma \gg 1$ ) charged particle appear more parallel and compressed in the direction transverse to the particle's motion, due to the Lorentz contraction. As seen from a target, this field looks like a pulse of a plane wave. But plane waves contain all electric and magnetic multipoles with the same weight. This is the cause for the equality between the virtual photon numbers as  $\gamma \rightarrow \infty$ .

In the limit of large frequencies  $\omega \gg \gamma v/R$  an adiabatic cutoff sets in and instead of (2.5) we have

$$n_{nl} \propto e^{-2\xi}. \quad (2.6)$$

This means that a useful approximation for some practical purposes is to use the relation (2.5) for  $\xi \leq 1$ , and  $n_{nl}(\omega) = 0$  for  $\xi > 1$ . In other words, the spectrum contains virtual photons with energies up to

$$(E_\gamma)_{\max} \approx \gamma \frac{\hbar v}{R}. \quad (2.7)$$

For a typical value of  $R = 10$  fm one obtains  $(E_\gamma)_{\max} \approx 20\gamma$  MeV.

For general purposes, the utility of eq. (2.1) is twofold: (a) if one multipolarity is favoured in a certain reaction, then by measuring the total Coulomb reaction cross section one can get information about the respective photo-induced process; (b) if the experimental data on the photo-induced process are available, one can use (2.1) to calculate the contribution of the electromagnetic interaction to the same process in a RHIC. The procedure (a) was indeed used in refs. <sup>7,10</sup> for two distinct aims. In this article we make a study of the relevance of the Coulomb induced processes in RHIC by means of the approach (b). For more details about the virtual photon theory see e.g. refs. <sup>1,6,7</sup>.

### 3. Electromagnetic nuclear excitation

In high energy collisions the electromagnetic excitation is a very sudden process and the excited states concentrate in a narrow region around the so-called giant resonances. These resonances will mostly decay by particle emission, or by fission in the case of very heavy nuclei like uranium. A direct break-up of the nuclei is also possible [see e.g. ref. <sup>10</sup>]. We can make some estimates of the contribution of each multipolarity to this process by using some theoretical sum rules for the excitation of giant resonances in the heavy ions. For simplicity we shall only treat the cases of the electric dipole and the electric quadrupole excitations. But, of course, one can directly include other multipoles if necessary.

In heavy nuclei the E1 and E2 giant resonances are peaked around the energies <sup>11)</sup>

$$E_{GR}^{(1)} = 80/A^{1/3} \text{ MeV}, \quad (3.1a)$$

$$E_{GR}^{(2)} = 62/A^{1/3} \text{ MeV}. \quad (3.1b)$$

To a good approximation we can take the factors  $n_{E1}(\omega)$  and  $n_{E2}(\omega)$  outside the integrals in (2.1)

$$\sigma_{CF} \approx \frac{n_{E1}[E_{GR}^{(1)}]}{E_{GR}^{(1)}} \int \sigma_{\gamma}^{E1}(E_{\gamma}) dE_{\gamma} + n_{E2}[E_{GR}^{(2)}] E_{GR}^{(2)} \int \frac{\sigma_{\gamma}^{E2}(E_{\gamma}) dE_{\gamma}}{(E_{\gamma})^2} \quad (3.2)$$

and make use of the sum rules<sup>11)</sup>

$$\int \sigma_{\gamma}^{E1}(E_{\gamma}) dE_{\gamma} \approx 60 \frac{NZ}{A} \text{ MeV} \cdot \text{mb}, \quad (3.3a)$$

$$\int \frac{\sigma_{\gamma}^{E2}(E_{\gamma})}{(E_{\gamma})^2} dE_{\gamma} \approx 0.22 ZA^{2/3} \mu\text{b}/\text{MeV}. \quad (3.3b)$$

Within these approximations the dependence of the Coulomb fragmentation cross sections  $\sigma_{CF}$  on the energy of the projectile  $E_{lab}$  is due to the dependence of  $n_{E1}$  and  $n_{E2}$  on that parameter. In fig. 1 we plotted the Coulomb fragmentation cross section  $\sigma_{CF}$  for  $^{238}\text{U}$  nuclei by means of  $^{40}\text{Ca}$  projectiles as a function of the laboratory energy per nucleon. For the nuclear parameter  $R$  we used

$$R = R_1 + R_2 = 1.2(A_1^{1/3} + A_2^{1/3}) \text{ fm}. \quad (3.4)$$

The dashed line corresponds to the E1 fragmentation mode and the dash-dotted line to the E2 one. The solid line is the sum of the two contributions. We note that the Coulomb fragmentation cross section overcomes the geometrical cross section  $\sigma_N = \pi(R_1 + R_2)^2$  for very high energies. One also observes that the E2 fragmentation mode is very important at intermediate energies (some hundreds of

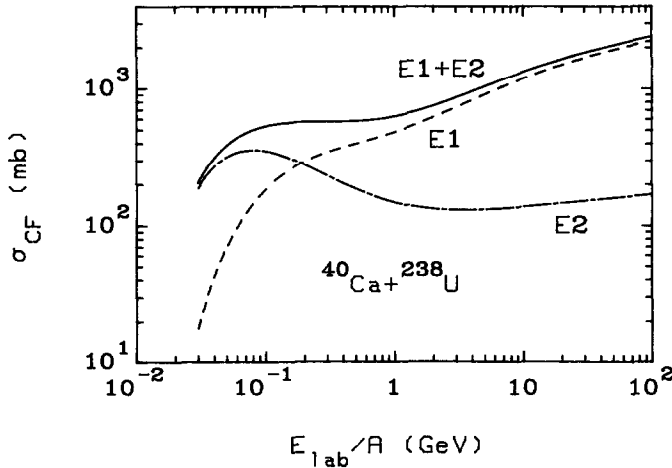


Fig. 1. Coulomb fragmentation cross section of  $^{238}\text{U}$  by means of relativistic  $^{40}\text{Ca}$  projectiles as a function of the laboratory energy per nucleon. The dashed line corresponds to the contribution of the giant electric dipole excitation to the fragmentation. The dash-dotted curve is the contribution of the giant electric quadrupole excitation and the solid curve is the sum of these two contributions.

MeV/nucleon) and even for very high energies it can account for approximately 10% of  $\sigma_{CF}$ . The excitation of giant magnetic dipole resonances in RHIC is of less importance since for intermediate energies  $n_{M1} \ll n_{E1}$  ( $n_{M1} \approx (v/c)^2 n_{E1}$ ) and for higher energies where  $n_{M1} \approx n_{E1}$  the cross section for the process will be smaller than that for the E1 case by the relative strength of the two giant resonances  $\sigma^{M1}/\sigma^{E1} \approx (\mu_N/eR_i)^2 = (\hbar/2m_N cR_i)^2 \ll 1$ , where  $m_N$  is the nucleon mass.

Experimental observation of Coulomb fragmentation in RHIC was obtained by the groups of the Lawrence Berkeley Laboratory and the Ames Laboratory [see e.g. refs. <sup>12,13</sup>]. If one could improve those experiments it would be a nice way for extracting information about the different decay modes of the nuclei through the excitation of giant resonances. The total photonuclear cross section is given by

$$\sigma_\gamma = \sum_l (\sigma_\gamma^{E_l} + \sigma_\gamma^{M_l}). \quad (3.5)$$

Normally, only a few multipoles contribute to a given process. Then by experimentally determining the total Coulomb excitation cross section in RHIC at different experimental conditions (e.g. by varying the beam energy) and using eq. (2.1) one will obtain a simple set of linear algebraic equations which can be solved to give the contributions of each multipolarity to the equivalent photonuclear process in (3.5). Of course, the method will not work for those processes in which  $n_{E1} \approx n_{M1} = n$  since then  $\sigma_C \approx \int n(\omega) \sigma_\gamma(\omega) d\omega/\omega$  and the separation of the multipoles will not be possible.

It has been suggested <sup>14</sup>) that one could have information on the different contributions of the M1 and of the E2 excitation of a nucleon to a  $\Delta$ -resonance by measuring the total Coulomb cross section for this process in a collision of a nucleon with a high- $Z$  nucleus at relativistic energies in the same way as was done in the CERN experiment to determine the lifetime of the  $\Sigma^0$  particle <sup>15,7</sup>). But, since the excitation energy of  $\hbar\omega \approx 300$  MeV is quite large, implying that  $\omega R/c \approx 15$  (for  $R \approx 10$  fm), then  $n_{E2}/n_{M1} \approx 1$  [see ref. <sup>7</sup>)] and the separation of the M1 and E2 contributions will be quite difficult in that approach.

The relations (2.2) were calculated on the basis of the first order perturbation theory <sup>6</sup>). In principle, this is a good approximation since, roughly speaking, the Coulomb interaction time in a RHIC is so short that one expects at most one virtual photon can be exchanged. In the time-dependent perturbation theory this means that the excitation amplitudes must be much smaller than one to justify the use of a first order perturbation method. In connection with Coulomb excitation in RHIC that question was nicely discussed in ref. <sup>5</sup>). But the possibility of multiple excitation in RHIC would be of great experimental interest. We calculated the probability amplitude for exciting a giant dipole resonance on a nucleus ( $Z_2, A_2$ ) by means of the Coulomb interaction with a projectile ( $Z_1, A_1$ ) in the case at which it could be as large as possible, namely when the impact parameter  $b$  is equal to the sum of the two nuclear radii  $R = R_1 + R_2$ . By using the TRK sum rule <sup>11</sup>) for the E1 resonance

and relating to the excitation amplitudes as given by eq. (2.15) of ref. <sup>5)</sup> we find

$$|a_{if}|_{m=0} \approx 0.41 \alpha \frac{Z_1 \sqrt{N_2 Z_2}}{A_2^{2/3}} \left( \frac{c}{\gamma v} \right)^2 K_0(\xi), \quad (3.6a)$$

$$|a_{if}|_{m=\pm 1} \approx 0.29 \alpha \frac{Z_1 \sqrt{N_2 Z_2}}{A_2^{2/3}} \frac{c^2}{\gamma v^2} K_1(\xi), \quad (3.6b)$$

where  $m$  is equal to the angular momentum transfer along the beam direction. In fig. 2 we plot  $a_0 \equiv |a_{if}|_{m=0}$  and  $a_1 \equiv |a_{if}|_{m=\pm 1}$  for the excitation of  $^{16}\text{O}$  in the reaction  $^{208}\text{Pb} + ^{16}\text{O}$ , and of  $^{238}\text{U}$  in the reaction  $^{238}\text{U} + ^{238}\text{U}$  as a function of the laboratory energy per nucleon. We observe that in both cases  $a_0$  decreases with increasing laboratory energy while  $a_1$  reaches a constant value. This occurs because  $a_0$  corresponds to excitation generated by a pulse of light in the direction perpendicular to the ion beam while  $a_1$  corresponds to another pulse in the beam direction. For high energies the first pulse becomes negligible and only the second one is important [see ref. <sup>1)</sup>, p. 719]. One also notes that the Coulomb excitation (mainly  $a_1$ ) of light systems like  $^{16}\text{O}$  by heavy ions has a small amplitude, while the same is not true

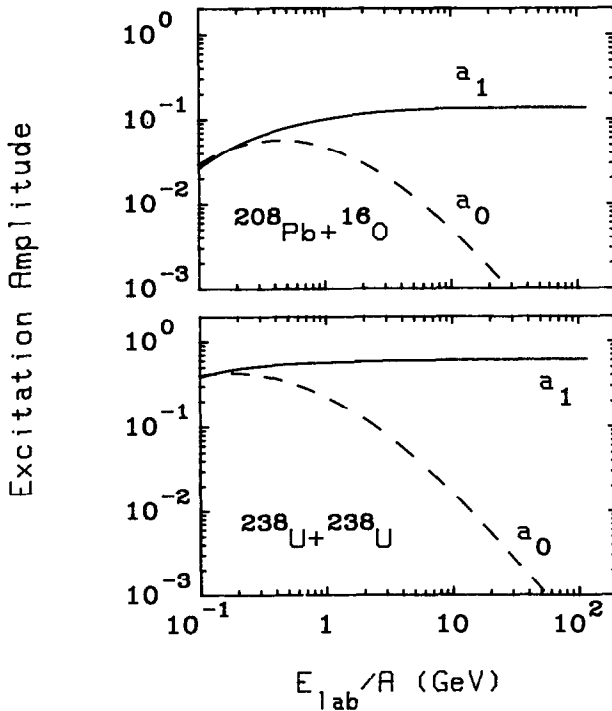


Fig. 2. Amplitudes for excitation of the giant electric dipole resonance of  $^{16}\text{O}$  and  $^{238}\text{U}$  by means of the Coulomb interaction with relativistic  $^{208}\text{Pb}$  and  $^{238}\text{U}$  projectiles, respectively, as a function of the laboratory energy per nucleon. The amplitude  $a_{0(1)} = |a_{if}|_{m=0(1)}$  corresponds to an angular momentum transfer of zero (one) unit in the direction parallel to the beam from the relative motion to the target.

for a heavy system like  $^{238}\text{U}$ . We took the smallest possible impact parameter; for larger impact parameters the excitation amplitudes will diminish. Nevertheless, a study of the role of multiple excitation in RHIC is worthwhile.

A very interesting subject is that concerning pion production in RHIC. The produced pions are supposed to be a source of information of the violent hadronic processes occurring in the central collisions. As implied by the relation (2.7) more and more virtual photons become available for energies  $E_\gamma \geq 140$  MeV corresponding to the photonuclear pion threshold, as one goes to higher beam energies. Above this energy the total photonuclear cross section is dominated by pion production and can be approximately written as

$$\sigma_{\gamma X} = A_{\text{eff}}(\omega) \left[ \frac{Z}{A} \sigma_{\gamma, \text{proton}}(\omega) + \frac{N}{A} \sigma_{\gamma, \text{neutron}}(\omega) \right]. \quad (3.7)$$

Experimentally it is found that  $A_{\text{eff}}$  is approximately independent of  $\omega$ , and shows a pronounced shadowing effect  $A_{\text{eff}} \approx A^{0.9}$ . We assume, for simplicity,

$$\sigma_{\gamma, \text{proton}} \approx \sigma_{\gamma, \text{neutron}} \equiv \sigma_{\gamma p}. \quad (3.8)$$

Then, pion production in RHIC through the Coulomb interaction can be approximately written as

$$\begin{aligned} \sigma(XY \rightarrow \pi XY) = & \int_{0.14 \text{ GeV}}^{\infty} n_1(E_\gamma) A_2^{0.9} \sigma_{\gamma p}(E_\gamma) \frac{dE_\gamma}{E_\gamma} \\ & + \int_{0.14 \text{ GeV}}^{\infty} n_2(E_\gamma) A_1^{0.9} \sigma_{\gamma p}(E_\gamma) dE_\gamma / E_\gamma, \end{aligned} \quad (3.9)$$

where  $n_1$  corresponds to the virtual photon spectrum generated by the nucleus X and that will cause the production of pions by the interaction with nucleus Y, and  $n_2$  corresponds to the inverse case. We use  $\pi l = M1$  since the pions are mostly produced through the nucleonic excitation to a  $\Delta$ -state which we assume to be of magnetic dipole origin. But the exact treatment of the multipolarity in this process is unimportant since for the relevant virtual photon energies which lead to pion production the virtual photon numbers are all approximately given by eq. (2.5). We used the experimental data of ref. <sup>16)</sup> for  $\sigma_{\gamma p}$ . The result of the integrations in (3.9) is shown in fig. 3 for the reactions  $^{40}\text{Ca} + ^{40}\text{Ca}$  and  $^{238}\text{U} + ^{238}\text{U}$  as a function of  $\gamma$  (roughly  $E_{\text{lab}}/A_1 \approx \gamma$  GeV for  $\gamma \gg 1$ ). There is a steep increase of the cross sections until a stage where they increase approximately proportional to  $(A_1 Z_2^2 + A_2 Z_1^2) \ln \gamma$ . The cross sections at this stage are quite large and for very heavy systems like  $^{238}\text{U} + ^{238}\text{U}$  it even can compete with those arising from hadronic interactions. The main difference is that while in a given Coulomb collision ( $b > R_1 + R_2$ ) the pion multiplicity can be at most one, in a central collision a large amount of pions can be produced. On the other hand, in relativistic heavy ion colliding beam accelerators the ion beams circle and collide many times before they are ready to be used in a

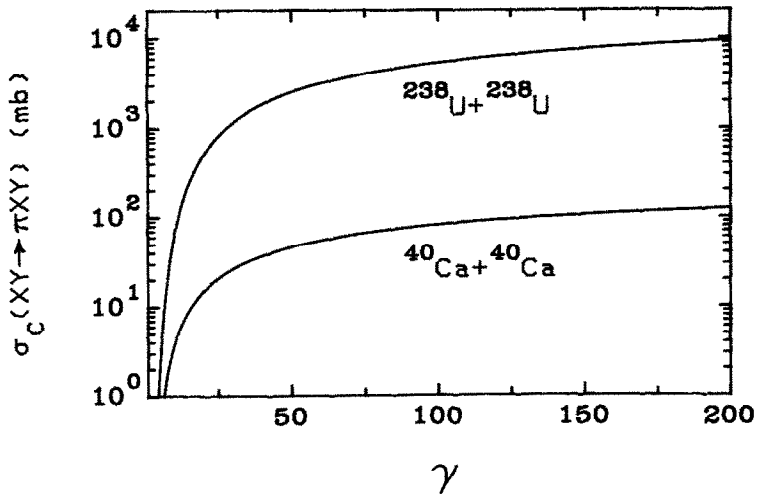


Fig. 3. Coulomb production cross sections of pions for the reactions  $^{40}\text{Ca} + ^{40}\text{Ca}$  and  $^{238}\text{U} + ^{238}\text{U}$  as a function of the relativistic Lorentz factor  $\gamma$ .

certain experiment. In these cases, the Coulomb interaction can produce an undesirable cloud of pions around the beams which might lead to experimental difficulties.

Pion production by means of Coulomb interaction was recently<sup>17)</sup> studied for carbon-carbon collisions below 300 MeV/nucleon. There it was concluded that this process is of minor importance for explaining the data on subthreshold pion production. The fact that pion production by means of electromagnetic interaction can only be important for higher beam energies is immediately clear from fig. 3.

#### 4. Bremsstrahlung

The emission of  $\gamma$ -rays in RHIC will be an important diagnostic tool for the time development of the nuclear collision [see e.g. refs. <sup>18,19)</sup>]. We will investigate the bremsstrahlung process for Coulomb collisions ( $b > R_1 + R_2$ ). This could be a potential source of background to be considered in possible experiments. A unique feature of this bremsstrahlung effect is the interference of the radiation from target and projectile. This will be specially important at low values of  $\gamma$ , it leads particularly to the well known vanishing of the E1 bremsstrahlung for systems with  $Z_1/M_1 = Z_2/M_2$ . In contrast to the low-energy case the emission of Coulomb bremsstrahlung at relativistic energies will be predominantly of E1 origin.

In accord with eq. (14.67) of ref. <sup>1)</sup> the energy radiated per unit solid angle per unit frequency interval is given classically by

$$\frac{d^2 I}{d\omega d\Omega} = \frac{e^2 \omega^2}{4\pi^2 c} |\mathbf{A}_1 + \mathbf{A}_2|^2, \quad (4.1)$$

where  $E_\gamma = \hbar\omega$  is now the energy of a real photon and

$$\mathbf{A}_i = Z_i \int_{-\infty}^{\infty} \hat{\mathbf{n}} \times \left( \hat{\mathbf{n}} \times \frac{\mathbf{v}_i}{c} \right) e^{i\omega(t - \hat{\mathbf{n}} \cdot \hat{\mathbf{r}}_i/c)} dt, \quad (4.2)$$

where  $i=1(2)$  refers to the projectile (target) labels,  $\mathbf{r}_i(\mathbf{v}_i)$  are their respective positions (velocities), and  $\hat{\mathbf{n}}$  is the direction of emission of the photon. By expanding eq. (4.1) the first (second) term corresponds to the radiation emitted by the projectile (target) and the third term to the interference between the two previous ones. Let us first discuss the radiation emitted by the target, assumed to be the laboratory system of reference.

The electric field at the position of the target and at time  $t$  when the projectile passes by with an impact parameter  $b$  is

$$E_z = -\frac{Z_1 e \gamma v t}{[b^2 + \gamma^2 v^2 t^2]^{3/2}}, \quad (4.3a)$$

$$E_t = \frac{Z_1 e \gamma b}{[b^2 + \gamma^2 v^2 t^2]^{3/2}}, \quad (4.3b)$$

where the  $z(t)$  indices denote the direction parallel (transverse) to the velocity of the projectile. In the laboratory system the target has a non-relativistic motion and we can use the dipole approximation <sup>1)</sup>

$$\begin{aligned} \left( \frac{d^2 I}{d\omega d\Omega} \right)_2 &\approx \frac{Z_2^2 e^2}{4\pi^2 c^3} \left| \int_{-\infty}^{\infty} \hat{\mathbf{n}} \times (\hat{\mathbf{n}} \times \dot{\mathbf{v}}_2) e^{i\omega t} dt \right|^2 \\ &= \frac{Z_2^2 e^4}{4\pi^2 M_2^2 c^3} |\hat{\mathbf{n}} \times \hat{\mathbf{n}} \times [E_z(\omega) + E_t(\omega)]|^2, \end{aligned} \quad (4.4)$$

where  $M_2$  denotes the target rest mass and  $E_z(\omega)$ ,  $E_t(\omega)$  are the Fourier transforms of the electric fields of eqs. (4.3). Expanding the triple vector product in (4.4) we obtain

$$\left( \frac{d^2 I}{d\omega d\Omega} \right)_2 = \frac{Z_1^2 Z_2^4 e^6 x^2}{\pi^2 M_2^2 c^3 b^2 v^2} \left\{ (1 - \cos^2 \theta) \frac{1}{\gamma^2} K_0^2(x) + (1 - \sin^2 \theta \sin^2 \phi) K_1^2(x) \right\}, \quad (4.5)$$

where  $x = \omega b / \gamma v$  and  $(\theta, \phi)$  are the angular coordinates of  $\hat{\mathbf{n}}$ .

The relation between (4.5) and the differential cross section for emission of bremsstrahlung radiation is

$$\left( \frac{d\sigma_{\text{br}}}{dE_\gamma} \right)_2 = \frac{1}{E_\gamma} \int_{b=R}^{b=\infty} \left( \frac{d^2 I}{dE_\gamma d\Omega} \right)_2 d^2 b d\Omega. \quad (4.6)$$

Both integrations can be done analytically and the final result can be written as

$$\left( \frac{d\sigma_{\text{br}}}{dE_\gamma} \right)_2 = \frac{8\pi}{3} \left( \frac{Z_2^2 e^2}{M_2 c^2} \right)^2 \frac{1}{E_\gamma} n_{\text{br}}^{(2)}(E_\gamma), \quad (4.7)$$

where  $n_{br}^{(2)}(E_\gamma)$  is equal to the virtual photon number  $n_{E1}$  as given by eq. (2.2a) with  $Z = Z_1$ . The result (4.7) has a very interesting interpretation: the emission of bremsstrahlung by the target (or by the projectile) can be viewed as the rescattering of the virtual photons generated by the projectile (target). The bremsstrahlung cross section is then given by the product of the virtual photon number per unit energy, given by  $n_{E1}(E_\gamma)/E_\gamma$ , and the classical Thomson cross section  $\sigma_T = \frac{8}{3}\pi(Z^2e^2/Mc^2)^2$ .

To calculate the radiation emitted by the projectile we can use (4.5) for the radiation emitted in the frame of reference of the projectile by interchanging the indices 1 and 2. Then we make a Lorentz transformation of  $d^2I/d\omega d\Omega$ ,  $\omega$  and  $\theta$  to the corresponding variables in the laboratory system (see eqs. (11.30) and (15.5) of ref. 1). We then obtain

$$\left(\frac{d^2I}{d\omega d\Omega}\right)_1 = \frac{Z_1^4 Z_2^2 e^6 x^2}{\pi^2 M_1^2 c^3 b^2 v^2} \{ [(1 - \beta \cos \theta)^2 - (\cos \theta - \beta)^2] K_0^2(y) + [\cos^2 \phi (1 - \beta \cos \theta)^2 + (\cos \theta - \beta)^2] K_1^2(y) \}, \tag{4.8}$$

where  $\beta = v/c$  and  $y = \gamma x(1 - \beta \cos \theta)$ . Integrating (4.8) in the same way as in (4.6) one finds

$$\left(\frac{d\sigma_{br}}{dE_\gamma}\right)_1 = \frac{8\pi}{3} \left(\frac{Z_1^2 e^2}{M_1 c^2}\right)^2 \frac{1}{E_\gamma} n_{br}^{(1)}(E_\gamma), \tag{4.9}$$

where

$$n_{br}^{(1)}(E_\gamma) = \frac{3}{4\pi} Z_2^2 \alpha \left(\frac{c}{v}\right)^2 \xi^2 \int_{-1}^1 du \left\{ \left[ 1 - \left(\frac{u - \beta}{1 - \beta u}\right)^2 \right] \frac{1}{\gamma^2} (K_1^2 - K_0^2) + \frac{1}{2} \left[ 1 + \left(\frac{u - \beta}{1 - \beta u}\right)^2 \right] (K_0 K_2 - K_1^2) \right\}, \tag{4.10}$$

with the  $K_\nu$  as functions of  $\chi = \gamma\xi(1 - \beta u)$  and  $u = \cos \theta$ . This last integration has to be solved numerically.

The radiation emitted by the projectile interferes with that from the target. To calculate it we have to expand the expression

$$\left(\frac{d^2I}{d\omega d\Omega}\right)_3 = \frac{e^2 \omega^2}{4\pi^2 c} (\mathbf{A}_1^* \cdot \mathbf{A}_2 + \mathbf{A}_1 \cdot \mathbf{A}_2^*). \tag{4.11}$$

To that aim we rewrite  $\mathbf{A}_1$

$$\mathbf{A}_1 \approx \frac{iZ_1}{\omega} \int_{-\infty}^{\infty} \frac{\hat{\mathbf{n}} \times [(\hat{\mathbf{n}} - \boldsymbol{\beta}) \times \dot{\boldsymbol{\beta}}]}{(1 - \boldsymbol{\beta} \cdot \hat{\mathbf{n}})^2} e^{i\omega t(1 - \beta \cos \theta)} dt \tag{4.12}$$

We then use  $\boldsymbol{\beta} = \beta \hat{\mathbf{z}}$  in the laboratory system. We also calculate  $\dot{\boldsymbol{\beta}}$  in the projectile system of reference by the action of the fields given by (4.3). Transforming  $\dot{\boldsymbol{\beta}}$  to the laboratory system, the integration in (4.12) can be solved analytically. The

amplitude  $A_2$  is simpler to calculate as already shown in eq. (4.4) and (4.5). Inserting  $A_1$  and  $A_2$  obtained in that way in eq. (4.11) we find

$$\left(\frac{d^2 I}{d\omega d\Omega}\right)_3 = -\frac{2Z_1^3 Z_2^3 e^6 \omega^2}{\pi^2 \gamma^2 M_1 M_2 c^3 v^4} \frac{1}{1 - \beta \cos \theta} \left\{ (1 - \cos^2 \theta) \frac{1}{\gamma^3} K_0(x) K_0(y) + \frac{1}{2} (1 + \cos^2 \theta - 2\beta \cos \theta) K_1(x) K_1(y) \right\}. \quad (4.13)$$

Integrating (4.13) in the same way as in (4.6) one finds

$$\left(\frac{d\sigma_{br}}{dE_\gamma}\right)_3 = -\frac{8\pi}{3} \left(\frac{Z_1 Z_2 e^2}{\sqrt{M_1 M_2} c^2}\right)^2 \frac{1}{E_\gamma} n_{br}^{(3)}(E_\gamma), \quad (4.14)$$

where

$$n_{br}^{(3)}(E_\gamma) = -\frac{3}{\pi} Z_1 Z_2 \alpha \frac{1}{\gamma} \left(\frac{c}{v}\right)^2 \xi \int_{-1}^1 \frac{du}{[(1 - \beta u)^2 - (1/\gamma^2)](1 - \beta u)} \times \left\{ \frac{1 - u^2}{\gamma^3} \left[ (1 - \beta u) K_0(\xi) K_1(\chi) - \frac{1}{\gamma} K_1(\xi) K_0(\chi) \right] + \frac{1}{2} (1 + u^2 - 2\beta u) \left[ (1 - \beta u) K_1(\xi) K_0(\chi) - \frac{1}{\gamma} K_0(\xi) K_1(\chi) \right] \right\}. \quad (4.15)$$

For  $Z_1 = Z_2$  and  $\gamma \rightarrow 1$  we obtain that  $n_{br}^{(3)} = n_{br}^{(1)} + n_{br}^{(2)}$  which expresses the well-known result of absence of bremsstrahlung dipole radiation for Coulomb collisions of particles with equal charge-to-mass ratio.

In fig. 4 we show  $n_{br}^{(i)}$  (for  $i=1$  solid line, for  $i=2$  dashed line, and for  $i=3$  dash-dotted line) as a function of the ratio between the nuclear dimension  $R$  and the real photon wavelength and for several values of  $\gamma$ . We used  $Z_1 = Z_2 = 10$ . One observes that  $n_{br}^{(3)}$  becomes smaller in comparison to  $n_{br}^{(1)}$  and  $n_{br}^{(2)}$  as  $\gamma$  increases. In the limit  $\gamma \rightarrow \infty$ ,  $n_{br}^{(3)} \rightarrow 0$ . This means that the radiations emitted by the projectile and by the target do not interfere with each other as  $\gamma \rightarrow \infty$ . It occurs because the recoil of the projectile is not instantaneously preceded by the recoil of the target as in the non-relativistic case. For relativistic energies the recoil of the nuclei is displaced in time by the retardation which leads to the incoherent emission of radiation. Also, in that limit the radiation emitted by a projectile is more intense than the one emitted by the target. This is because photons of energy  $E'_\gamma$  in the projectile system of reference, emitted approximately isotropically, appear in the laboratory within a forward cone  $\theta_{max} \approx 1/\gamma$  and with energies of the order of  $E_\gamma \approx \gamma E'_\gamma$ , i.e. energetic photons in the laboratory system come from soft photons in the frame of reference of the projectile [see e.g. ref. <sup>1</sup>].

A more violent source of bremsstrahlung radiation has its origin in the collision with  $b < R_1 + R_2$  where part of the charges carried by the projectile almost comes into stop. To compare the relevance of these two different mechanisms of producing bremsstrahlung, i.e. the Coulomb and the nuclear one, we use the results of ref. <sup>18</sup>)

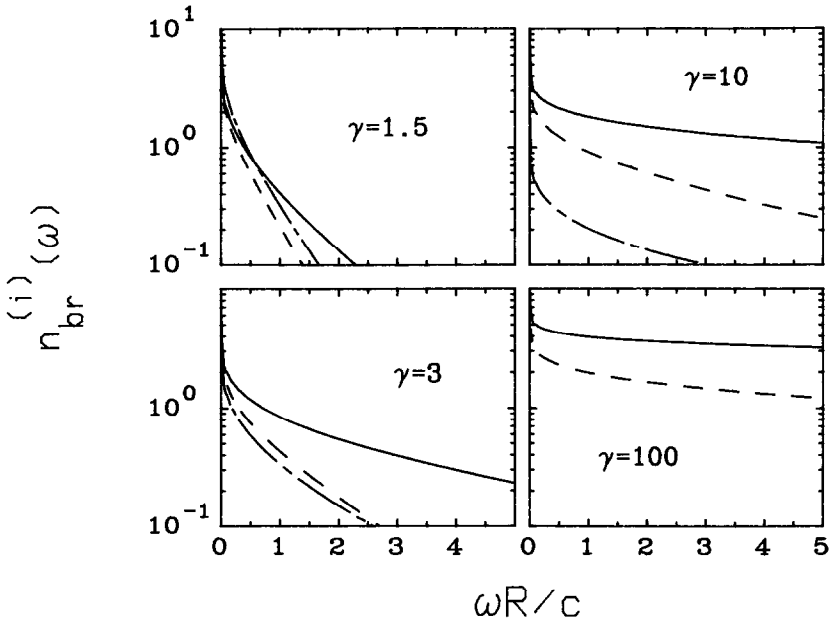


Fig. 4. The adimensional bremsstrahlung strength functions  $n_{br}^{(i)}$  (see text) plotted against the ratio between the nuclear dimension  $R$  and the photon wavelength for several values of  $\gamma$ .

where the nuclear bremsstrahlung in RHIC was calculated on the basis of a nuclear fireball model which accounts for the possible formation of two fireballs. Integrating eq. (5) of that reference with respect to the solid angle we obtain (for the special case of symmetrical systems, i.e.,  $Z_1 = Z_2 = Z$ )

$$\left(\frac{d\sigma}{dE_\gamma}\right)_{Nbr} = \frac{1.9 + \sqrt{2}}{28} \frac{Z^2 \alpha R^2}{E_\gamma} \{F(\beta) + F(\beta_{PF}) + F(\beta_{TF}) - 2[G(\beta, \beta_{PF}) + G(\beta, \beta_{TF}) - G(\beta_{PF}, \beta_{TF})]\}, \quad (4.16a)$$

where

$$F(\beta) = \frac{1}{\beta} \ln\left(\frac{1+\beta}{1-\beta}\right) - 2 \quad (4.16b)$$

$$G(\beta, \beta_F) = \frac{\beta\beta_F}{2(\beta - \beta_F)} \left\{ \frac{1 - \beta_F^2}{\beta_F} F(\beta_F) - \frac{1 - \beta^2}{\beta} F(\beta) + 2(\beta - \beta_F) \right\} \quad (4.16c)$$

with  $\beta_{PF}$  and  $\beta_{TF}$  respectively equal to the projectile and target fireball velocity as given by eq. (6) of ref. <sup>18</sup>). We used in that equation the transparency factor  $\eta$  equal to 75%. We define the dimensionless quantity

$$r(\gamma, E_\gamma) = \frac{(d\sigma/dE_\gamma)_{Nbr}}{(d\sigma/dE_\gamma)_{Cbr}}, \quad (4.17)$$

TABLE 1

Ratio of nuclear and Coulomb bremsstrahlung cross sections for the reaction  $^{40}\text{Ca} + ^{40}\text{Ca}$  and  $E_\gamma = 10$  MeV; the value of  $E_\gamma(d\sigma/dE_\gamma)_{\text{Nbr}}$  is also given

$\gamma$	$r(\gamma, E_\gamma = 10 \text{ MeV})$	$E_\gamma(d\sigma/dE_\gamma)_{\text{Nbr}}(\text{mb})$
1.1	$2.6 \times 10^2$	$5.1 \times 10^{-2}$
1.5	$5.3 \times 10^5$	0.69
10	$1.0 \times 10^6$	18.5
100	$1.5 \times 10^6$	27.7

where the Coulomb bremsstrahlung cross section  $(d\sigma/dE_\gamma)_{\text{Cbr}}$  is given by the sum of eqs. (4.7), (4.9) and (4.14). In table 1 we show  $r(\gamma, E_\gamma)$  for the reaction  $^{40}\text{Ca} + ^{40}\text{Ca}$  and  $E_\gamma = 10$  MeV. One observes that only for low values of  $\gamma$  (in which case Coulomb repulsion corrections to the trajectory must be taken into account) the Coulomb bremsstrahlung is relevant. Also, for greater values of  $E_\gamma$  the ratio  $r$  increases.

Coulomb bremsstrahlung seems to be of little relevance in RHIC. Its role increases for collisions of less massive particle like electron or muon-nucleus scattering and, e.g., could be useful for obtaining information on the elastic scattering of photons on unstable particles, like pions. For example, in the process  $Z + \pi \rightarrow Z + \pi + \gamma$  one could study the scattering of photons on pions, this could yield a value of the pion polarizability via the Rayleigh scattering amplitude, which increases in importance as compared to the Thomson scattering term (see eq. (4.7)) with increasing  $\gamma$ -energy.

## 5. K-shell ionization

Ionization of K-shell atomic electrons by means of relativistic particles is a subject of increasing interest [see e.g. ref. <sup>20</sup>]. We will limit our analysis to the cross sections for ionization of a given target by means of relativistic heavy ions. Opposite to heavy ion scattering at nonrelativistic energies, in the relativistic case K-shell ionization is favoured as compared to L, M, etc. ionization of the atoms of a dense target as the ions penetrate it. In ref. <sup>21</sup>) a simple expression for these cross sections was obtained by separating the ionization into those arising from close and distant collisions. The contribution from distant collisions was calculated by replacing the field of the incident ion by a spectrum of virtual photons and multiplying it with the photoelectric cross section. The contribution from close collisions was based on the binary encounter approximation which assumes that for high beam energies the atomic electrons can be regarded as free. The total cross section can be written as

$$\sigma_K = \sigma_{b \leq a_K} + \sigma_{b > a_K}, \quad (5.1)$$

where  $a_K$  is the K-shell radius and  $\sigma_{b > a_K}$  and  $\sigma_{b \leq a_K}$  are given by the equations (18) and (22) of that paper, respectively.

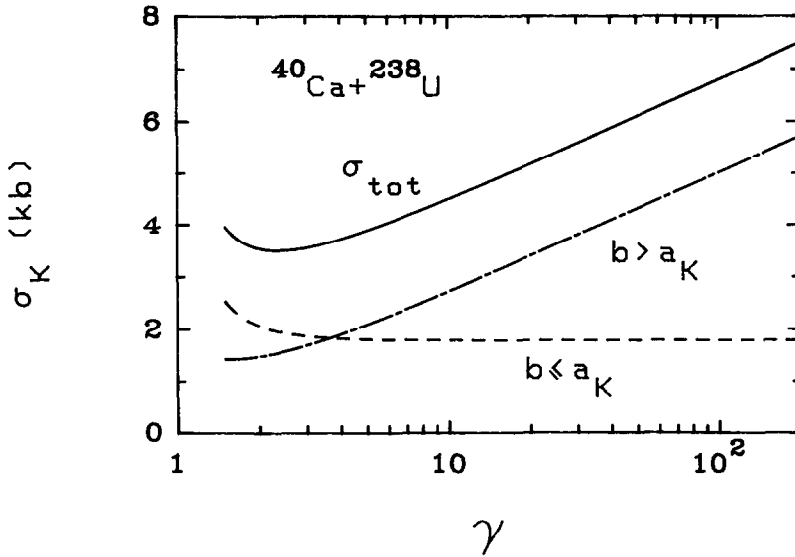


Fig. 5. Cross section for atomic K-shell ionization of  $^{238}\text{U}$  by means of relativistic  $^{40}\text{Ca}$  projectiles as a function of the Lorentz factor  $\gamma$ . The dashed (dash-dotted) curve corresponds to the contribution of impact parameters smaller (larger) than the K-shell radius. The solid curve is the sum of the two contributions.

In fig. 5 we show the cross section for K-shell ionization of  $^{238}\text{U}$  targets by means of relativistic  $^{40}\text{Ca}$  projectiles as a function of  $\gamma$ . One sees that for great values of  $\gamma$  the contribution of distant collisions  $\sigma_{b > a_K}$  is larger than that from close collisions  $\sigma_{b \leq a_K}$  which tends to a constant value as  $\gamma \rightarrow \infty$ . In that limit, the virtual photon theory alone can account for the main features of the cross sections. As soon as the K-shell electrons are most tightly bound the photoelectric cross section is largest and preferentially K-holes are formed.

Since the ionization cross sections are large, the relativistic heavy ion ionization could perhaps be used as a variant of the well-known PIXE<sup>22)</sup> technique for the analysis of materials.

## 6. Electron-pair production and stopping power

Since the photon energy necessary to produce an  $e^+e^-$  pair in the field of a nucleus is quite small ( $E_\gamma \geq 1$  MeV) it must be a process of great importance in RHIC. The pair production due to the electromagnetic interaction in a collision between the nuclei X and Y is given by

$$\begin{aligned} \sigma(XY \rightarrow e^+e^-XY) = & \int_{2m_e c^2}^{\infty} n_1(E_\gamma) \sigma(\gamma X \rightarrow e^+e^-X) \frac{dE_\gamma}{E_\gamma} \\ & + \int_{2m_e c^2}^{\infty} n_2(E_\gamma) \sigma(\gamma Y \rightarrow e^+e^-Y) \frac{dE_\gamma}{E_\gamma}. \end{aligned} \quad (6.1)$$

For simplicity we use with good approximation the cross section for pair production by real photons in the field of a nucleus  $A$ , in the case of complete screening by the atomic electrons, given by<sup>23)</sup>

$$\sigma(\gamma A \rightarrow e^+ e^- A) = \frac{28}{9} Z^2 r_0^2 \alpha \left[ \ln \left( \frac{183}{Z^{1/3}} \right) - \frac{1}{42} - f(Z) \right], \quad (6.2a)$$

where  $r_0 = e^2/m_e c^2$  is the classical electron radius and  $f(Z)$  is a correction to the plane wave Born approximation

$$f(Z) = (Z\alpha)^2 \sum_{n=1}^{\infty} \frac{1}{n(n^2 + Z^2\alpha^2)}. \quad (6.2b)$$

We also use (2.5) for the virtual photon numbers in (6.1) and, instead of infinity, we set the adiabatic cutoff (2.7) in the upper limit of the integrals in (6.1). The result can be expressed analytically and, in the special case of identical nuclei ( $Z_1 = Z_2 = Z$ ;  $A_1 = A_2 = A$ )

$$\sigma(AA \rightarrow e^+ e^- AA) \approx Z^2 \alpha \frac{2}{\pi} \left\{ \left[ \ln \frac{2\alpha R}{\delta \gamma r_0} \right]^2 - [\ln(1/\delta)]^2 \right\} \sigma(\gamma A \rightarrow e^+ e^- A). \quad (6.3)$$

In fig. 6 we plotted the cross sections for  $e^+ e^-$  pair production in RHIC due to the electromagnetic interaction for the collision of  $^{40}\text{Ca} + ^{40}\text{Ca}$  and  $^{238}\text{U} + ^{238}\text{U}$  as obtained from eq. (6.3). One observes a logarithmic increase with the energy and also a great enhancement of the cross sections with the charge number of the systems involved. This comes from the approximate  $Z_1^2 Z_2^2$  dependence of the cross sections. Like in the case of pion production the  $e^+ e^-$  pair production in RHIC will lead to

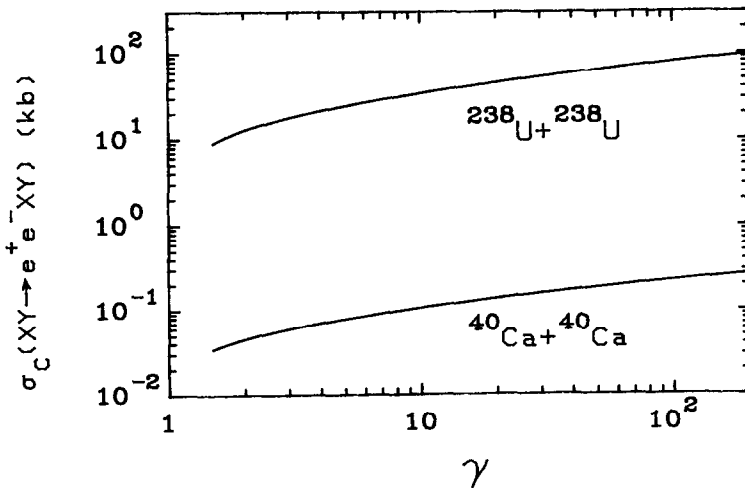


Fig. 6. Cross sections for Coulomb production of electron-positron pairs in the relativistic heavy ion collisions of  $^{40}\text{Ca} + ^{40}\text{Ca}$  and  $^{238}\text{U} + ^{238}\text{U}$  as a function of the Lorentz factor  $\gamma$ . Note that the ordinate is given in kilobarns.

the formation of a cloud of electrons (and positrons) accompanying the beams in relativistic heavy ion accelerators. This might also be a cause of experimental difficulties.

One common characteristic of atomic ionization and of  $e^+e^-$  pair production is the very large value of the cross sections. Although the energy transferred to the atomic electron or to the  $e^+e^-$  pair is generally small one still can expect that they can cause a great energy loss of the projectiles as they penetrate a dense medium. The energy loss per unit length will be given by

$$-\left(\frac{dE}{dx}\right) = \rho \int_{(E_\gamma)_{\min}}^{(E_\gamma)_{\max}} E_\gamma \frac{d\sigma}{dE_\gamma} dE_\gamma, \quad (6.4)$$

where  $\rho$  is the number of atoms per unit volume of the medium. In the case of atomic ionization  $(E_\gamma)_{\min}$  is equal to the ionization energy  $I$  and  $(E_\gamma)_{\max}$  is set to  $2m_e c^2 \gamma^2 \beta^2$  for  $b \leq a_K$  and to  $\gamma \hbar c / a_K$  for  $b > a_K$ . By using the equation for  $d\sigma/dE_\gamma$  as given in ref. <sup>21)</sup> we obtain

$$-\left(\frac{1}{E} \frac{dE}{dx}\right)_{b \leq a_K} = 4\lambda_N^{-1} Z_1^2 \left(\frac{r_0}{R}\right)^2 \frac{1}{\gamma\beta^2} \left(\frac{m_e}{m_N}\right) \frac{1}{A_1} \left\{ \frac{I}{2\beta\gamma^2} + \ln\left(\frac{2\gamma^2\beta^2}{I}\right) - \beta \right\}, \quad (6.5)$$

where  $m_N$  is the nucleon mass and  $I$  is given in units of  $m_e c^2$ . The quantity

$$\lambda_N = \frac{1}{\rho\sigma_N} = \frac{1}{\pi\rho(R_1 + R_2)^2} \quad (6.6)$$

is equal to the mean-free-path of the projectile if it only would interact with the target by means of nuclear forces. The contribution from  $b > a_K$  gives

$$-\left(\frac{1}{E} \frac{dE}{dx}\right)_{b > a_K} \approx 1.39 \frac{Z_1^2}{Z_2^2 \alpha^2} \left(\frac{r_0}{R}\right)^2 \lambda_N^{-1} \frac{I}{E} \left\{ (1 - q^2 + 2q^3) \ln \left[ \left(\frac{\delta}{q}\right)^2 \right] - [q^3(\frac{1}{3} - \ln q) - 2q^2(\frac{1}{2} - \ln q)] \right\}, \quad (6.7)$$

where  $q = Ia_K / \gamma \hbar v$ .

The contribution to the stopping power due to  $e^+e^-$  pair production can be calculated in the same way as before by using eq. (2.5) and the cutoff (2.7). This leads to

$$-\left(\frac{1}{E} \frac{dE}{dx}\right)_{e^+e^-} = \frac{4}{\pi^2} Z_1^2 \alpha \lambda_N^{-1} \frac{m_e c^2}{ER^2} \sigma(\gamma A_2 \rightarrow e^+ e^- A_2) \times \left\{ \ln \frac{2m_e c^2 R}{\delta \gamma \hbar v} - 1 + \frac{\gamma \hbar v}{2m_e c^2 R} (\ln \delta + 1) \right\}. \quad (6.8)$$

The contribution to the stopping power coming from  $e^+e^-$  pair production in the nuclear field of the projectile is obtained from (6.8) by interchanging the variables corresponding to the projectile and the target. But the atomic ionization of the projectile or the pair production in the nuclear field of the projectile by an amount

of energy  $\Delta E$  contributes to an energy loss of the order of  $\gamma\Delta E$  from the relative motion. The total energy loss is then given by

$$\frac{dE}{dx} = \gamma \left( \frac{dE}{dx} \right)_1 + \left( \frac{dE}{dx} \right)_2, \tag{6.9}$$

where  $(dE/dx)_{1,2}$  is obtained by summing eqs. (6.5), (6.7) and (6.8) for the projectile (target). In fig. 7 we plot  $-(1/E) dE/dx$  in units of  $\lambda_N^{-1}$  for relativistic  $^{208}\text{Pb}$  nuclei incident on a  $^{208}\text{Pb}$  target. The dashed curve represents the contribution from atomic collisions and the dash-dotted curve is the contribution from pair production. The solid curve is given by eq. (6.9). We observe that in contrast to low-energy collisions, where atomic ionization predominates, in RHIC the main contribution to the electromagnetic stopping power comes from  $e^+e^-$  pair production. In the ultrarelativistic limit  $\gamma \gg 1$  it tends to a linear function of  $\gamma$

$$-\left( \frac{1}{E} \frac{dE}{dx} \right)_{e^+e^-} = \frac{2}{\pi^2} \frac{Z_2^2}{A_1} \alpha \lambda_N^{-1} \gamma \left( \frac{\hbar}{m_N c R^3} \right) (\ln \delta + 1) \sigma(\gamma A_1 \rightarrow e^+e^- A_1). \tag{6.10}$$

In fig. 8 we show the stopping power due to  $e^+e^-$ -pair production of  $^{238}\text{U}$  ions as they penetrate several targets, in units of  $\lambda_N^{-1}$ . One notes that for very high beam

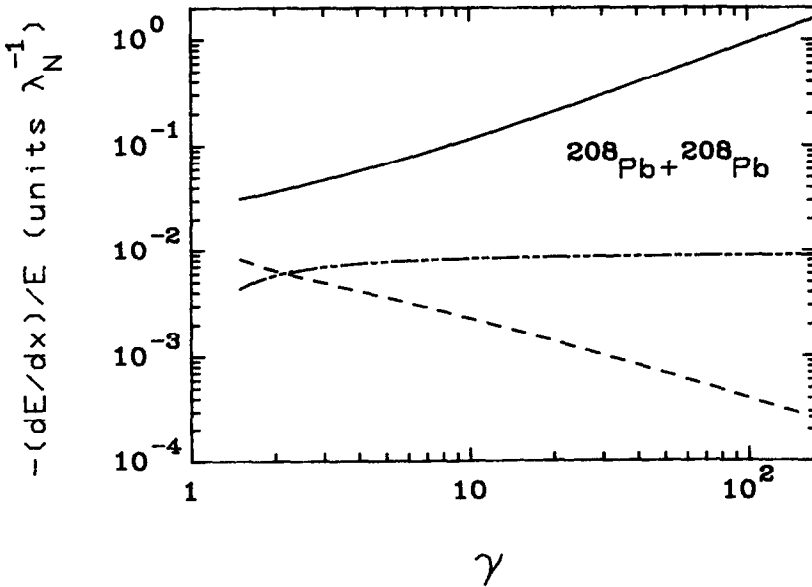


Fig. 7. Coulomb stopping power of  $^{208}\text{Pb}$  projectiles as they penetrate a  $^{208}\text{Pb}$  target in units of the inverse of the nuclear mean free path  $\lambda_N$  (see text) and as a function of the Lorentz factor  $\gamma$ . The dashed curve corresponds to energy loss due to atomic K-shell ionization. The dash-dotted curve corresponds to the energy loss due to  $e^+e^-$  pair production in the target region. The solid curve is the sum of the contributions of atomic ionization and  $e^+e^-$  pair production in the projectile and in the target as given by eq. (6.9).

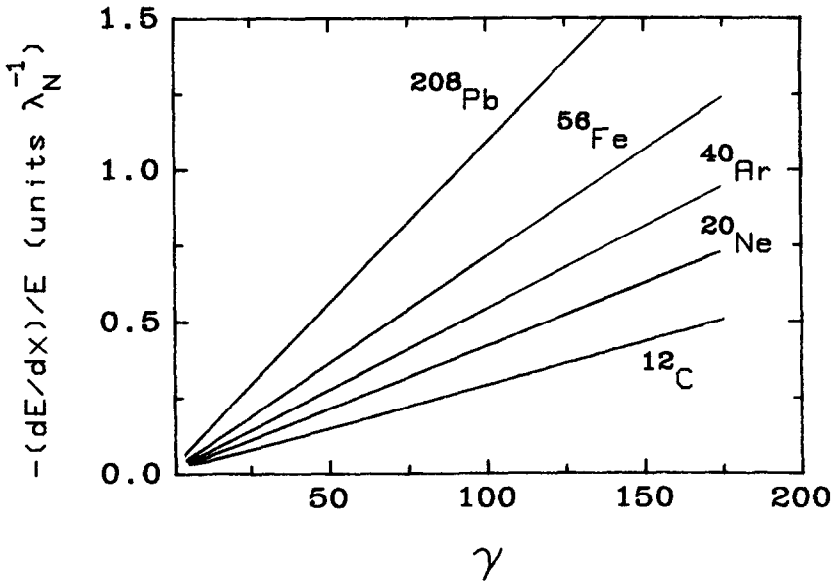


Fig. 8. Coulomb stopping power of  $^{238}\text{U}$  projectiles as they penetrate several dense targets in units of the inverse of nuclear mean free path  $\lambda_N$  and as a function of the Lorentz factor  $\gamma$ . Only the energy loss due to  $e^+e^-$  pair production is taken into account.

energies the stopping power due to  $e^+e^-$  pair production is comparable to that originating from pure nuclear interactions.

## 7. Conclusions

Electromagnetic effects in RHIC are very important and interesting. Since the electromagnetic interaction is well known reliable theoretical predictions are possible. The method of virtual photons has proven to be a very powerful and transparent tool to study these effects. It allows a clear separation into a purely kinematical aspect (virtual photon number) and a cross section for a process induced by real photons. Since with an increasing value of the relativistic parameter  $\gamma$  the hardness of the virtual photons is increased, many new possibilities open up. Thus it becomes possible to excite strongly collective high-lying nuclear states (GMR), a process which has already been observed and which is theoretically well understood. With increasing  $\gamma$ , pion production will become important, it has been quantitatively calculated in this paper, based on our knowledge of pion production in  $\gamma$ -nucleus interactions. Bremsstrahlung, the elastic scattering of virtual photons on charged particles, is relatively unimportant for the heavy ions, although interesting effects are also to be observed in this field. K-shell ionization will be large; most prominent will be the strong  $e^+e^-$  pair production. It will also contribute significantly to the RHI stopping power. Since the electric field of a heavy ion is  $Z$  times stronger than

the field of a particle with charge  $e$  (like  $e$ ,  $\mu$ ,  $p$ ), it is in some cases a very useful source of virtual photons. Apart from the interest of electromagnetic effects in RHIC for their own sake, it will be important to take these effects with large cross sections into account in the considerations of building RHI machines as well as in the design of experiments whose main aim will be the study of nuclear matter under extreme conditions.

We want to thank Prof. A. Winther for interesting discussions.

This work was partially supported by the Deutscher Akademischer Austauschdienst/CAPES.

### References

- 1) J.D. Jackson, *Classical electrodynamics* (Wiley, New York, 1975)
- 2) E. Fermi, *Z. Phys.* **29** (1924) 315
- 3) C.F. Weizsäcker, *Z. Phys.* **88** (1934) 612
- 4) E.J. Williams, *Phys. Rev.* **45** (1934) 729
- 5) A. Winther and K. Alder, *Nucl. Phys.* **A319** (1979) 518
- 6) C.A. Bertulani and G. Baur, *Nucl. Phys.* **A442** (1985) 739
- 7) C.A. Bertulani and G. Baur, *Phys. Rev.* **C33** (1986) 910
- 8) Proc. Third Int. Conf. on ultra-relativistic nucleus-nucleus collisions, Brookhaven National Laboratory, September 1983, ed. by T.W. Ludlam and H.E. Wegner, in *Nucl. Phys.* **A418** (1984)
- 9) C.A. Bertulani, Proc. Workshop on Gross properties of nuclei and nuclear excitations, Hirschegg, Austria, January 1986
- 10) G. Baur, C.A. Bertulani and H. Rebel, *Nucl. Phys.* **A458** (1986) 188
- 11) See e.g. A. Bohr and B. Mottelson, *Nuclear structure*, vol. II (Benjamin, Reading, MA, 1975)
- 12) D.L. Olson, B.L. Berman, D.E. Greiner, H.H. Heckman, P.J. Lindstrom, G.D. Westfall and H.J. Crawford, *Phys. Rev.* **C24** (1981) 1529
- 13) M.T. Mercier, J.C. Hill, F.K. Wahn and A.R. Smith, *Phys. Rev. Lett.* **52** (1984) 898
- 14) J. Wambach, private communication
- 15) F. Dydak, F.L. Navarria, O.E. Overseth, P. Steffen, J. Steinberger, H. Wahl, E.G. Williams, F. Eisele, C. Geweniger, K. Kleinknecht, H. Taureg and G. Zech, *Nucl. Phys.* **B118** (1977) 1
- 16) T.A. Armstrong *et al.*, *Phys. Rev.* **D5** (1972) 1640
- 17) J.W. Norbury and L.W. Townsend, *Phys. Rev.* **C33** (1986) 337
- 18) J.I. Kapusta, *Phys. Rev.* **C15** (1977) 1580
- 19) J.D. Bjorken and L. McLerran, *Phys. Rev.* **D31** (1985) 63
- 20) B.L. Moiseiwitsch, *Phys. Reports* **118** (1985) 133
- 21) F. Komarov, *Radiation Effects* **46** (1980) 39
- 22) T.A. Cahill, *Ann. Rev. Nucl. Part. Sci.* **30** (1980) 211
- 23) A.I. Akhiezer and V.B. Berestetskii, *Quantum electrodynamics* (Wiley, New York, 1965)